NASA TT F-11,467

WIDE-BAND QUASI-OPTIC PRISM COMPONENTS

T. Sueta, N. Kumagai and S. Kurazono

Translation of an article from the Journal of the
Institute of Electrical Communication Engineers of Japan
Vol. 49, No. 3, pp. 457-462, 1966

NATIONAL AERONAUTICS AND SPACE ADMINISTRATION
WASHINGTON, D.C. 20546 JANUARY 1968

WIDE-BAND QUASI-OPTIC PRISM COMPONENTS

T. Sueta[†], N. Kumagai[††] and S. Kurazono[††]

ABSTRACT: A quasi-optic directional coupler, attenuator, and magic T which use a dielectric prism matchable over a wide range of bands are proposed. The principle of wide-band matching and the operational characteristics are described. The result of experiments in the 50 Gc band showed an excellent agreement of the experimental and calculated values, confirming that these components have better characteristics than any of this type previously reported. It is believed that the quasi-optic component described in this paper can be applied to a wide range of frequencies from short millimeter and sub-millimeter waves to that of the coherent optical wave region which has recently been developed.

1. INTRODUCTION

/457*

In order to put a free-space transmission system such as a beam waveguide into practical use in the region of the millimeter waves and below, it becomes necessary to develop components suitable for such a system.

This paper takes up the fixed or variable directional coupler, the fixed or variable reactance attenuator, and the magic T, all of which employ the dielectric prism, as components that satisfy such a requirement. The paper also examines the principle of wide-band matching and its operational characteristics, both theoretically and experimentally.

[†] Faculty of Engineering Science, Osaka University, Osaka.

[††] Faculty of Engineering, Osaka University, Osaka.

* Numbers in the margin indicate pagination in the foreign text.

The idea of quasi-optic components that make use of the dielectric prism, such as those mentioned above, dates back even to an old work by Bose [1]. Since then, several works [2-6] have appeared on the subject. However, all of them have structures such that the electromagnetic waves are perpendicularly incident on each surface of the prism, giving rise to an undesirable reflection on each surface. Because of this, none of them possesses the excellent characteristics required for the components. For example, in the case of a directional coupler, the characteristics of the directional selectivity and the insertion-loss are restricted in principle due to the existence of the undesirable reflected waves. Furthermore, there is the disadvantage that frequency characteristics appear in the degrees of coupling and directional selectivity. To eliminate such undesirable reflected waves, a device such as quarter wavelength matching has been invented. However, the range of the matched frequency band of such a method is essentially narrow, so that its practical usefulness as a component becomes very limited.

In contrast to this, the matching method which uses the Brewster angle, proposed recently by Makimoto and Sueta [7,8], has the excellent advantage that it does not have (in principle) any frequency characteristics so long as the prism medium is non-dispersive. The only conceivable disadvantage of the matching method which uses the Brewster angle is that it imposes a restriction on the polarization direction of the wave. However, when it is actually applied to a reflection-type waveguide(for example), the above restriction on the polarization direction does not actually become a detriment which narrows the applicability of the component, since the low-loss transmitted beam wave is linearly polarized [9] in a certain direction initially.

In this paper, we will discuss the theoretical relationships which play the basic roles in wide-band matching using the Brewster angle. We will then present the principle of operation, an example of the design, and the operational characteristics, etc., of the fixed and variable directional coupler, the fixed and directional attenuator, and the magic T that employ a wide-band non-reflecting prism to which the above theory applies.

2. THEORETICAL CONSIDERATIONS

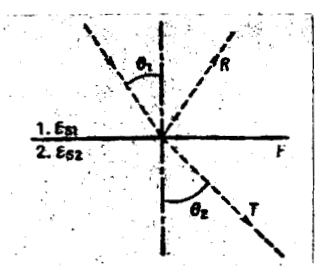

Fig. 1. Reflection and Transmission at a Plane Boundary between Two Different Dielectrics.

When a plane wave whose electric vector is to the boundary plane F of isotropic and lossless media 1 (specific dielectric constant ε_{s1}) and 2 (specific dielectric constant ε_{s2}) strikes an interface at an angle θ_1, the reflection and transmission coefficients R and T, respectively, of the electric power are given by the following expressions [10]:

$$\left.\begin{aligned} R&=\left|\frac{\sqrt{\varepsilon_{s1}}\cos\theta_1-\sqrt{\varepsilon_{s2}}\cos\theta_2}{\sqrt{\varepsilon_{s1}}\cos\theta_1+\sqrt{\varepsilon_{s2}}\cos\theta_2}\right|^2 \\ T&=1-R \end{aligned}\right\} \qquad (1)$$

where θ_2 represents the deflection angle. Furthermore, the following relation between θ_1 and θ_2 follows from Snell's law.

$$\sqrt{\varepsilon_{s1}}\sin\theta_1=\sqrt{\varepsilon_{s2}}\sin\theta_2 \qquad (2)$$

The incident angle θ_B for which $R \square 0$ is given by (1) as /458

$$\theta_B=\tan^{-1}\sqrt{\frac{\varepsilon_{s2}}{\varepsilon_{s1}}}\,. \qquad (3)$$

Such an angle θ_B is called the Brewster angle. As we see from (3), the Brewster angle θ_B is independent of frequency as long as the media are non-dispersive.

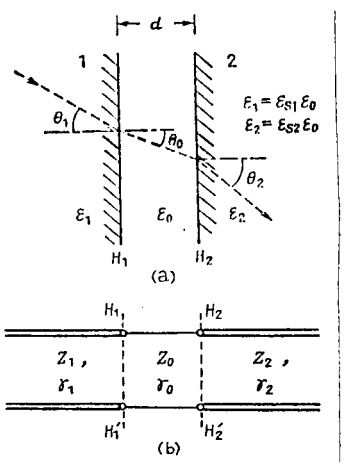

Fig. 2. Three-Layered Dielectric Medium (a), and its Equivalent Circuit Representation (b).

Let us next consider a case in which two dielectrics 1 and 2 and separated by a gap d, as shown in Fig. 2. For the calculation of the power reflection coefficient of the wave striking the interface through dielectric 1 and the power transmission coefficient from dielectric 1 to dielectric 2, we can think of a transmission line model which is equivalent to Fig. 2(a) and shown in Fig. 2(b) [11]. If we assume that the electric vector of the incident wave is parallel to the interface, the characteristic impedance Z and the propagation constant γ in the dielectrics and the gap are given by the following expressions, respectively:

$$\left.\begin{aligned} Z_i&=\eta\frac{1}{\sqrt{\varepsilon_{si}}}\cos\theta_i \\ \gamma_i&=j\frac{2\pi}{\lambda}\sqrt{\varepsilon_{si}}\cos\theta_i \end{aligned}\right\} \quad i=0,\ 1,\ 2 \qquad (4)$$

Here, λ denotes the wavelength in free space and $\eta = \sqrt{\mu_0/\varepsilon_0}$ is the characteristic impedance of free space. The remaining notations are as in Fig. 2. If we compute Z_0, γ_0 and Z_2 from the above equations for a case where θ_1 is greater than the critical angle θ_c ($\theta_c = \sin^{-1}\sqrt{1/\varepsilon_{s1}}$), we obtain

$$\left.\begin{aligned} Z_0&=jx=j\eta\sqrt{\varepsilon_{s1}\sin^2\theta_1-1} \\ \gamma_0&=\alpha=\frac{2\pi}{\lambda}\sqrt{\varepsilon_{s1}\sin^2\theta_1-1} \\ Z_2&=\eta\sqrt{\frac{1}{\varepsilon_{s2}}\left(1-\frac{\varepsilon_{s1}}{\varepsilon_{s2}}\sin^2\theta_1\right)} \end{aligned}\right\} \qquad (5)$$

where x and α are real numbers. On the other hand, the impedance matrix between H_1 and H_2 of Fig. 2(b) is given by

$$\begin{pmatrix} Z_{11} & Z_{12} \\ Z_{21} & Z_{22} \end{pmatrix} = Z_0 \begin{pmatrix} \coth \alpha d & \operatorname{cosech} \alpha d \\ \operatorname{cosech} \alpha d & \coth \alpha d \end{pmatrix}. \tag{6}$$

Hence, the power reflection coefficient R and the power transmission coefficient T for this case are given by the following expressions.

$$\left.\begin{aligned} R &= 1 - T \\ T &= \left| \frac{2\sqrt{Z_1 Z_2}\, Z_{12}}{(Z_{11}+Z_1)(Z_{22}+Z_2) - Z_{12}^2} \right|^2 \end{aligned}\right\} \tag{7}$$

We compute T by substitution in (4)-(6) as follows:

$$\frac{1}{T} = A \sinh^2 \alpha d + B \tag{8}$$

where

$$\left.\begin{aligned} A &= \frac{(\varepsilon_{s1}-1)(\varepsilon_{s2}-1)\{(\varepsilon_{s1}+1)\sin^2\theta_1 - 1\}\{\varepsilon_{s1}(\varepsilon_{s2}+1)\sin^2\theta_1 - \varepsilon_{s2}\}}{4\sqrt{\varepsilon_{s1}\varepsilon_{s2}}\cos\theta_1(\varepsilon_{s1}\sin^2\theta_1 - 1)\sqrt{\varepsilon_{s2} - \varepsilon_{s1}\sin^2\theta_1}} \\ B &= \frac{\{\varepsilon_{s2}\cos\theta_1 + \sqrt{\varepsilon_{s1}(\varepsilon_{s2} - \varepsilon_{s1}\sin^2\theta_1)}\}^2}{4\sqrt{\varepsilon_{s1}\varepsilon_{s2}}\cos\theta_1\sqrt{\varepsilon_{s2} - \varepsilon_{s1}\sin^2\theta_1}} \end{aligned}\right\}. \tag{9}$$

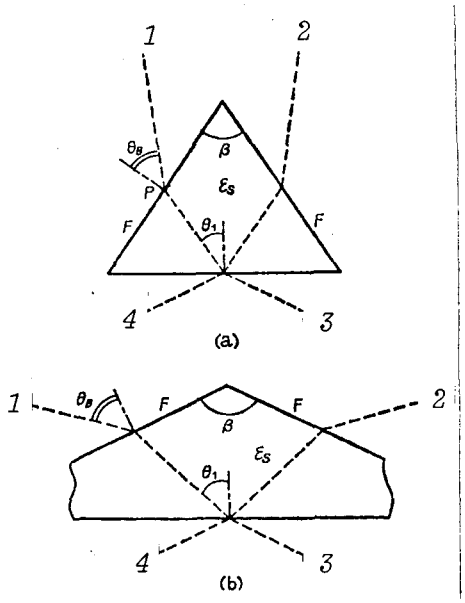

Fig. 3. Wide-Band Single-Prism Directional Couplers.

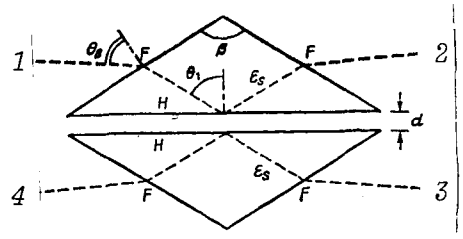

Fig. 4. Wide-Band Double-Prism Variable Directional Coupler.

In a special case, when the dielectric constants of the two dielectrics are equal ($\varepsilon_{s1} = \varepsilon_{s2} = \varepsilon_s$), (8) is valid with the following values of A and B:

$$\left.\begin{aligned} A &= \frac{(\varepsilon_s - 1)^2\{(\varepsilon_s+1)\sin^2\theta_1 - 1\}^2}{4\varepsilon_s\cos^2\theta_1(\varepsilon_s\sin^2\theta_1 - 1)} \\ B &= 1 \end{aligned}\right\} \tag{10}$$

As can clearly be seen from (1) and (8), it is possible to reflect or transmit the incident power in an arbitrary ratio by varying the angle of incidence θ_1 or the gap d. Figures 3 and 4 show examples of construction of fixed and variable directional couplers based on this principle. In these diagrams, the angle of incidence at surface F of each prism equals the Brewster angle given by (3), eliminating the undesirable reflection. As mentioned before, there will be no frequency characteristics in this matching method as long as the dielectric constant of the dielectric is non-dispersive.

/459

3. RESULT OF MEASUREMENTS OF CHARACTERISTICS OF THE VARIOUS COMPONENTS

3.1. Double-Prism Directional Coupler and Attenuator

The elements of the S-matrix of a double-prism variable directional coupler which uses two dielectric prisms with equal dielectric constants, as shown in Fig. 4, are obtained from (8) as follows:

$$\left.\begin{aligned} &S_{ii}=S_{14}=S_{23}=0,\ i=1,2,3,4 \\ &|S_{12}|^2=|S_{34}|^2=1-|S_{13}|^2 \\ &|S_{13}|^{-2}=|S_{24}|^{-2}=A\sinh^2\alpha d+B \end{aligned}\right\} \qquad (11)$$

Here

$$\alpha=\frac{2\pi}{\lambda}\sqrt{\varepsilon_s\sin^2\theta_1-1}$$

A and B are given by (10), and the other notations are as shown in Fig. 4. As we see from (11), we can achieve an arbitrary degree of coupling ($-10\log|S_{13}|^2$) by varying the gap d. The directional selectivity theoretically becomes ∞ dB.

An example of the result of the test on a design using the 50 Gc band is shown in Fig. 5. Teflon (specific dielectric constant ε_s = 2.12) was used as the prism material and the prisms were designed such that the condition of the Brewster angle on the surfaces F and the condition of total reflection on the surfaces H are satisfied. As a result, the angle θ_B, β, θ_1, etc. are given by

$$\theta_B=\tan^{-1}\sqrt{\varepsilon_s}=\tan^{-1}\sqrt{2.12}=55.5^\circ$$

(θ_B = Brewster angle)

$$\beta=2\theta_B=111^\circ,\quad \theta_1=\pi-2\theta_B=69^\circ$$

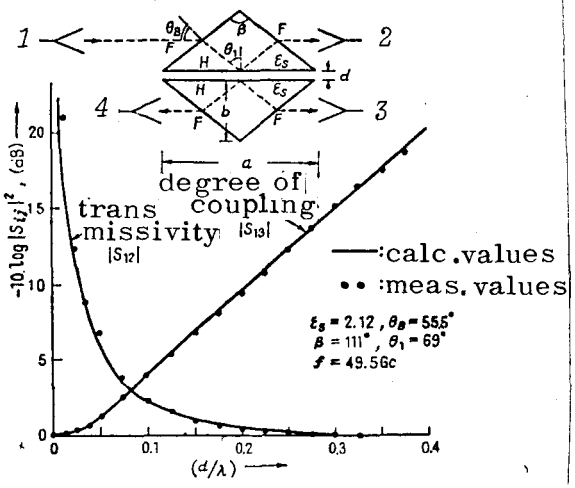

Fig. 5. Illustration of Measured (Dots) and Calculated (Solid Lines) Characteristics of Wide-Band, Double-Prism Variable Directional Coupler.

It is to be noted that the direction of polarization of the incident wave is assumed to be parallel to the plane of incidence; moreover, the design is such that the input and output waves become parallel. The dimensions of the prism are: a = 13.5 cm, b = 4.7 cm, and the thickness = 5 cm.

As the transmitter horn *1* we used Type 4011 (made by Hitachi); as the receiver horns *2-4* we used magnetic horns with aperture = 30 mm x 2.4 mm and length 50 mm. One of the two prisms is fixed and the other is movable relative to the former by a micrometer screw mechanism, and the gap d is read from the micrometer. The separation of the receiver horns *2-4* and the prism surface is set to about 1 cm, and the separation between the transmitter

horn *1* and the prism surface is set to more than 1 m in order to improve the applicability of the plane-wave approximation of the incident electromagnetic wave.

The black dots in Fig. 5 represent the measured values (at the frequency 49.5 Gc) of the coupling ($-10 \log|S_{13}|^2$) and transmissivity ($-10 \log|S_{12}|^2$) characteristics. The measured values (in dB) are those assumed by the output of the receiver horn *3* corresponding to zero separation d as the standard (0 dB). The solid lines in Fig. 5 are calculated values based on (11). As seen from the diagram, the agreement between the measured and calculated values is excellent. As may be seen from examples of the measured frequency characteristics for d = 0.3 mm and 1.2 mm, similar agreement is accomplished for other frequencies also.

The insertion-loss over the frequency band measured was about 0.2 dB. This value is close to the calculated value when tan δ of teflon is taken as 0.3×10^{-3}. To show the wide-band nature of matching with the use of the Brewster angle, in Fig. 7 we compared numerically the insertion-losses for the gap separation d = 0 in the case of prisms using the Brewster angle and in the case of right-angle prisms. Compared with the case of prisms using the Brewster angle, the case of right-angle prisms previously used shows that the insertion-loss exhibits marked frequency characteristics, with an increase of its value due to unwanted reflection at the input and output surfaces of the prisms. A similar situation takes place for cases where the gap separation is nonzero. /460

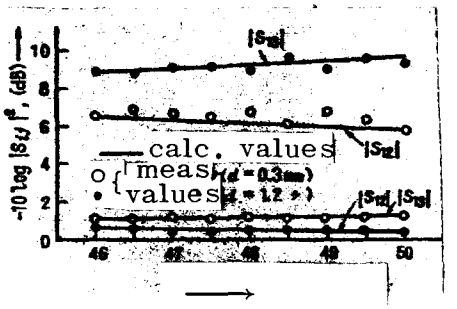

Frequency (Gc)

Fig. 6

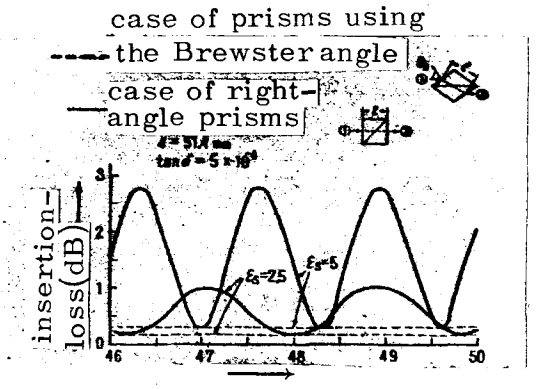

Frequency (Gc)

Fig. 7

Fig. 6. Frequency Characteristics of Wide-Band, Double-Prism Variable Directional Coupler. Measured (Dots) and Calculated (Solid) Line).

Fig. 7. Comparison of Insertion-Loss of Wide-Band, Double-Prism Variable Directional Coupler with That of Ordinary Rectangular Prism Coupler (Calculated).

Figure 8 shows the directional selectivity (the ratio of the output to *3* and the output to *4*) measured at the same frequency of 49.5 Gc. For comparison, we also show the directional selectivity characteristics of a double-prism directional coupler which does not use the Brewster angle, recently described by Fellers et al [6] in IEE Transactions on MTT (calculated values shown as a solid line). It can be seen that the trial coupler produced by the authors has far superior characteristics.

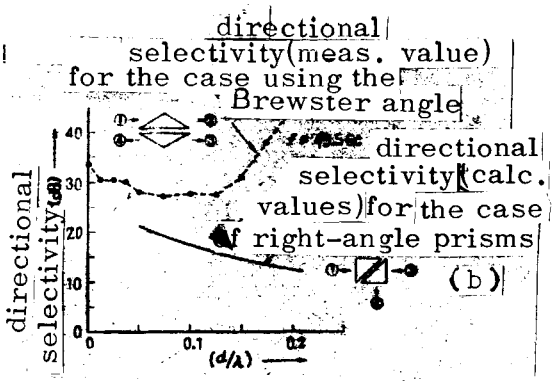

Fig. 8. Comparison of Directivity of Wide-Band, Double-Prism Variable Directional Coupler (Measured) with That of Ordinary Rectangular Prism Coupler (Calculated).

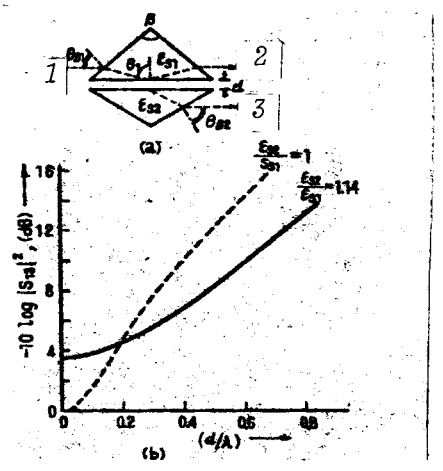

Fig. 9. Characteristics of Wide-Band, Double-Prism Variable Directional Couplers Using a Pair of Prisms Having Different (Solid Line) and Same (Broken Line) Dielectric Constants.

When a directional coupler is constructed from two kinds of dielectric prism with different dielectric constants as shown in Fig. 9(a), its S-matrix elements can be obtained from (11) by substituting (5) for α and (9) for A and B. Thus, for example, the degree of coupling for

$$\varepsilon_{s1} = 1.1,\ \varepsilon_{s2} = 1.254, \text{ and } \theta_1 = 87°16'$$

varies with the gap d as shown in the solid line of Fig. 9(b), and its variation with d is slower as compared to the case (broken line of the same figure) of a double-prism using the same kind of dielectrics ($\varepsilon_{s1} = \varepsilon_{s2} = 1.1$). Therefore, in order to realize precisely a degree of coupling of the order of several dB by a fine adjustment, it is advantageous in practice to use a double-prism which is composed of two dielectrics with different dielectric constants. However, in this case the degree of coupling for zero value of d does not become 0 dB. Instead, it reduces to a fixed directional coupler with a certain fixed degree of coupling which is determined by the ratio of the dielectric constants of the two kinds of dielectrics and the summit angle β of the prism.

The double-prisms shown in Figs. 4 and 9(a) can also be used as variable reactance attenuators. For example, if we regard *1* and *3* as the input and output termini, respectively, their characteristics are given by the curve for $|S_{13}|$ of Fig. 5 and Fig. 9(b), respect-

ively. Since these attenuators can be calibrated, theoretically they may be used as standard attenuators. In addition, the fact that the relationship between the gap d and the amount of attenuation shows very good linearity except for the neighborhood of $d = 0$ is a practical advantage. /461

3.2. Single-Prism Directional Coupler and Attenuator

When a single dielectric prism (as shown in Fig. 3) is used, it becomes a fixed directional coupler. It must be designed so that the condition of the Brewster angle is satisfied on the surface F to avoid unwanted reflection there. The S-matrix elements for this case are given from (1) by the following:

$$\left.\begin{aligned} &S_{ii}=S_{14}=S_{23}=0,\ i=1,2,3,4 \\ &|S_{13}|^2=|S_{24}|^2=1-|S_{12}|^2 \\ &|S_{12}|^2=|S_{34}|^2=\frac{\tan^2\{\theta_1-\sin^{-1}(\sqrt{\epsilon_s}\sin\theta_1)\}}{\tan^2\{\theta_1+\sin^{-1}(\sqrt{\epsilon_s}\sin\theta_1)\}} \end{aligned}\right\} \quad (12)$$

where

$$\theta_1 = \theta_B - \frac{\beta}{2} \quad : \text{Case of Fig. 3(a)}$$

$$\theta_1 = \pi - \theta_B - \frac{\beta}{2} \quad : \text{Case of Fig. 3(b)}$$

As seen from (12), the degree of coupling of such a single-prism directional coupler is a constant, independent of the frequency, determined by the summit angle β of the prism or θ_1.

Figure 10 shows the coupling characteristics of a single-prism fixed directional coupler which was designed and produced in trial form using teflon as the prism material ($\varepsilon_s = 2.12$) and with $\beta = 60°$, $\theta_1 = 25.5°$, length of one side = 12 cm, and thickness = 5 cm. Here, the measured values (black dots, in dB) represent the power received when its standard (0 dB) is taken as the case where the prism is removed and receiver horn *2* or *3* is placed at point P of Fig. 3(a) exactly opposite transmitter horn *1*. The solid line represents the calculated values based on (12). In these calculated values, the loss is taken into account by assuming tan δ of the dielectric to be equal to 0.3×10^{-3}.

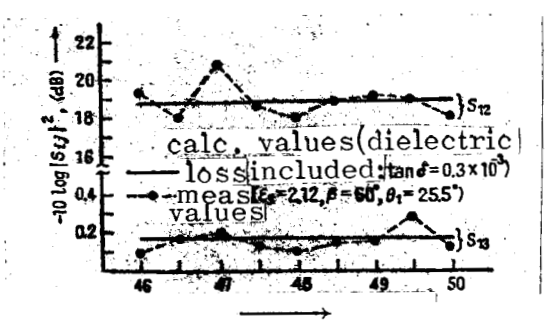

Fig. 10. Frequency Characteristics of Wide-Band, Single-Prism Directional Coupler. Measured (Dots) and Calculated (Solid Lines).

When the single prism mentioned above is used, it is obvious that we obtain a fixed attenuator with a definite amount of attenuation.

3.3. Magic T

In a double-prism directional coupler like the one in Fig. 4, if we adjust the gap so as to divide the input through *1* equally into *2* and *3*, it becomes equivalent to a magic T.

As an example, if we set (in the double-prism using Teflon) $\beta = 111°$, $\theta_1 = 69°$, $d = 0.51$ mm, and frequency $f = 49.5$ Gc, it becomes a magic T, and its separability becomes about 27.5 dB (measured value).

4. CONCLUSIONS

The principle and characteristics of a wide-band prism directional coupler, attenuator, and magic T which make use of the Brewster angle are discussed. It is shown that the results of trial production and experimentation in the 50 Gc band agree very well with the calculated values. It is believed that such components can be extended and applied not only to the short millimeter and sub-millimeter waves but also to the light wave region which has recently been developed.

Acknowledgement: We are deeply indebted to Professor Toshio Makimoto, Faculty of Engineering Science, Osaka University, who gave guidance and advice regarding the present research. We also wish to thank Professor Kiyoyasu Itakura, Faculty of Engineering, Osaka University who provided constant guidance, as well as Mr. Tsuneo Nakahara (Chief of the Electronics Section) and Mr. Noritaka Kurauchi, both from the Research Laboratory of Sumitomo Electric Works, who helped us in the preparation of the prisms. We thank Messrs. Hajime Onishi and Hiroaki Nishiyama who cooperated with us in carrying out the experiments.

REFERENCES

1. Bose, J.C.: Collected Physical Papers; London, Longmans Green, 1927.
2. Harvey, A.F.: Optical Techniques at Microwave Frequencies; Proc. Inst. Elec. Engrs. (London), Vol. 106B, p. 141, March 1959.
3. Fellers, R.G.: Millimeter Wave Transmission by Non-Waveguide Means; Microwave J., Vol. 5, No. 5, p. 80, May, 1962.
4. Raker, H.D. and G.R. Valenzuela: A Double-Prism Attenuator for Millimeter Waves; Inst. Radio Engrs., Trans., MTT-10, p. 392, September, 1962.
5. Hindin, H.J. and J.J. Taub: Oversize Waveguide Directional Coupler; Inst. Radio Engrs., Trans., MTT-10, p. 394, September, 1962.

6. Fellers, R.G. and J. Taylor: Internal Reflections in Dielectric Prisms; Inst. Elec. Electr. Engrs., Trans., MTT-12, p. 584, November, 1964.
7. Makimoto, T. and T. Sueta: Prism Directional Couplers Using the Brewster Angles; Research Data on Radiation Science, February, 1963.
8. Makimoto, T. and T. Sueta: Prism Directional Couplers Making Use of Brewster Angle Transmission; Mem. Inst. Sci. Ind. Research Osaka Univ., Vol. 21, 1964.
9. Kumagai, N., et al: Behavior of the Transmitted Beam of a Reflection Type Beam Waveguide; Research Data on Microwave Transmission, Inst. of Elect. Commun. Engs. Journal, July, 1945. /462
10. Stratton, J.A.: Electromagnetic Theory; New York, McGraw-Hill, 1941, NB Chapter 9.
11. Schelkunoff, S.A.: Electromagnetic Waves; New York, D. van Nostrand, 1943, NB Chapter 8.

APPENDIX

A.1. Brewster Angle Matching of Dielectric Prisms with High Dielectric Constant

In the design of various components which make use of dielectric prisms with high dielectric constant, if it is desired to achieve wide-band matching by use of the Brewster angle, it becomes impractical because the Brewster angle approaches 90°. In such a case, one can avoid inconvenience by inserting a dielectric prism 2 which has a dielectric constant between those of the two media 1 and 3 (as shown in Fig. A.1), to make the incident angles at each interface become the Brewster angles.

In the case of Fig. A.1(a), the summit angle ϕ of the intermediate prism 2 is given from the figure by the following expression.

$$\phi = 90° + \theta_{B2} - \theta_{B1} \tag{A.1}$$

where θ_{B1} and θ_{B2} stand for the Brewster angles at surfaces A and B, respectively. In the case of Fig. A.1(b), the summit angle ϕ of the intermediate prism 2 is given by the following:

$$\phi = \theta_{B1} + \theta_{B2} - 90°. \tag{A.2}$$

As a special case of $\theta_{B1} = \theta_{B2}$, we have $\phi = 90°$ in the setup shown in Fig. A.1(a). This means that we may use a right-angle prism as the intermediate prism. Furthermore, the incident direction on surface A and the transmitted direction on surface B become parallel in this case. The condition for $\theta_{B1} = \theta_{B2}$ is given by

$$\varepsilon_2 = \sqrt{\varepsilon_1 \varepsilon_3} \tag{A.3}$$

which is the same as the condition of matching by the use of a quarter-wavelength dielectric plate. Although there are frequency characteristics, in the case of a quarter-wavelength matching, the matching condition becomes independent of the frequency for a method like the one above which makes use of an intermediate prism, as long as the dielectric is non-dispersive.

A.2. Generalized Brewster Angle

The Brewster angles at the boundary surface of two kinds of media with different dielectric constants and magnetic permeability are given by the following. If we call the Brewster angles for the cases where the electric vector is perpendicular and parallel to the incident planes $\theta_{B\perp}$ and $\theta_{B\parallel}$, respectively, they are given by

$$\theta_{B\perp} = \cos^{-1}\sqrt{\frac{(\mu_2\varepsilon_2/\mu_1\varepsilon_1)-1}{(\mu_2/\mu_1)^2-1}} \tag{A.4}$$

$$\theta_{B\parallel} = \cos^{-1}\sqrt{\frac{(\mu_2\varepsilon_2/\mu_1\varepsilon_1)-1}{(\varepsilon_2/\varepsilon_1)^2-1}} \qquad (A.5)$$

In these equations ε_1, μ_1 and ε_2, μ_2 represent the dielectric constant and magnetic permeability of media 1 and 2, respectively. The conditions for the existence of $\theta_{B\perp}$ and $\theta_{B\parallel}$ are determined from (A.4) and (A.5) and are given in Table A.1. As seen from this table,

TABLE A.1. CONDITIONS OF EXISTENCE OF GENERALIZED BREWSTER ANGLES

	$\varepsilon_1<\varepsilon_2$		$\varepsilon_1>\varepsilon_2$	
	$\mu_1<\mu_2$	$\mu_1>\mu_2$	$\mu_1<\mu_2$	$\mu_1>\mu_2$
Existence Condition for $\theta_{B\perp}$	$\frac{\varepsilon_2}{\varepsilon_1} \leqq \frac{\mu_2}{\mu_1}$	$\mu_1\varepsilon_1 > \mu_2\varepsilon_2$	$\mu_1\varepsilon_1 < \mu_2\varepsilon_2$	$\frac{\varepsilon_2}{\varepsilon_1} \geqq \frac{\mu_2}{\mu_1}$
Existence Condition for $\theta_{B\parallel}$	$\frac{\varepsilon_2}{\varepsilon_1} \geqq \frac{\mu_2}{\mu_1}$	$\mu_1\varepsilon_1 < \mu_2\varepsilon_2$	$\mu_1\varepsilon_1 > \mu_2\varepsilon_2$	$\frac{\varepsilon_2}{\varepsilon_1} \leqq \frac{\mu_2}{\mu_1}$

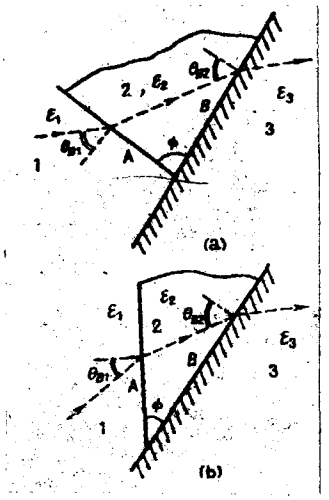

Fig. A.1. Technique to Perform the Wide-Band Matching Between Two Dielectric Media Having Significantly Different Dielectric Constants.

$\theta_{B\perp}$ and $\theta_{B\parallel}$ cannot exist simultaneously except for the case of the equality sign. However, when the equality sign holds, we obtain $\theta_{B\perp} = \theta_{B\parallel} = 0$, so that there is no sense in discriminating between the polarization directions. When the equality sign holds, the wave impedances $\sqrt{\mu/\varepsilon}$ of the two media become equal; hence, it is natural that there is no reflection for the incident wave which is perpendicular to the interface.

In the case of $\mu_1 = \mu_2$, there exists only $\theta_{B\parallel}$ which is given by

$$\theta_{B\parallel} = \cos^{-1}\sqrt{\frac{1}{(\varepsilon_2/\varepsilon_1)+1}} = \tan^{-1}\sqrt{\varepsilon_2/\varepsilon_1} \qquad (A.6)$$

which agrees with (3). Furthermore, for the case $\varepsilon_1 = \varepsilon_2$, only $\theta_{B\perp}$ exists and is given by

$$\theta_{B\perp} = \tan^{-1}\sqrt{\mu_1/\mu_2}. \qquad (A.7)$$

That is to say, by the use of a magnetic substance, we can make $R_\perp \doteq 0$. In this case, it can be applied for instance to parallel lines on a plate and so on, since the electric vector is perpendicular to the incident plane.

Translated for the National Aeronautics and Space Administration by: Aztec School of Languages, Inc.; Acton, Massachusetts
NASw-1692